

Article

Raman Scattering Study of Amino Acids Adsorbed on A Silver Nanoisland Film

Alexey Skvortsov^{1,2}, Ekaterina Babich^{3,4}, Andrey Lipovskii^{3,5,*}, Alexey Redkov⁶, Guang Yang⁷ and Valentina Zhurikhina³

¹Institute of Biomedical Systems and Biotechnology, Peter the Great St. Petersburg Polytechnic University, Polytechnicheskaya 29, 195251, St. Petersburg, Russia

²Laboratory of the Molecular Biology of Stem Cells, Institute of Cytology, Russian Academy of Sciences, Tikhoretsky 4, 194064, St. Petersburg, Russia

³Institute of Physics and Mechanics, Peter the Great St. Petersburg Polytechnic University, Polytechnicheskaya 29, 195251, St. Petersburg, Russia

⁴Laboratory of Nanophotonics, Alferov University, Khlopina 8/3, 194021, St. Petersburg, Russia

⁵Department of Physics and Technology of Nanostructures, Alferov University, Khlopina 8/3, 194021, St. Petersburg, Russia

⁶Institute for Problems in Mechanical Engineering of the Russian Academy of Sciences, Bolshoy prospekt V.O. 61, 199178, St. Petersburg, Russia

⁷School of Materials Science and Engineering, Shanghai University, Shangda Rd. 99, Baoshan, Shanghai 200444, China

Abstract

We studied surface enhanced Raman spectra of amino acids *D*-alanine and *DL*-serine and their mixture on silver nanoisland films (SNF), immersed in phosphate buffer saline solution at millimolar amino acid concentrations. It is shown that the spectra from the amino acid solutions differ from the reference spectra for microcrystallites due to electrostatic orientation of amino acid zwitterions by the metal nanoisland film. Moreover, non-additive peaks are observed in the spectrum of the mixture of amino acids adsorbed on SNF, which means that intermolecular interactions between adsorbed amino acids are very significant. The results indicate the need for a thorough analysis of the Raman spectra from amino acid solutions in the presence of a nanostructured metal surface, and may also be of interest for studying molecular properties and intermolecular interactions.

Keywords: SERS; metal surfaces; amino acids

1. Introduction

Surface enhanced Raman scattering (SERS) of organic molecules by surface plasmon resonance (SPR) of metallic structures and surfaces is a promising sensing technique, which has gained considerable interest in the recent decades [1]. Metal particles are often used in SERS, as they are more expendable, easy to produce, and can provide larger enhancement than bulk metal [2]. There is a large amount of data on excellent sensitivity and temporal resolution of SPR biosensors, which allows detection of single molecules [3], runtime measurements [4], microscopic hyperspectral imaging [5] and other. However, surface chemistry plays a very

*Corresponding author: lipovsky@spbau.ru

important role in the formation of SERS spectra. In general, patterns and regularities observed in a bulk solution Raman spectra cannot be extrapolated to SERS spectra of an analyte adsorbed by a metal surface [6], and thorough studies are required. Multiplexed sensing of several analytes by SERS also raises questions of difference in adsorption of an analyte on the metallic surface and interaction of different analytes at the surface.

One of the promising SERS substrates for biosensing applications are silver nanoisland films (SNF), which can be produced by out-diffusion of a metal from glass substrates [7]. It was shown previously that SNF can enhance the Raman spectra of various molecules [8, 9]. We have recently shown that SNFs formed by out-diffusion are not inherently stable in phosphate buffer saline solution (PBS), which is widely used in biochemical and cell studies, and other buffer systems [10]. The film gradually reacts with the medium releasing silver ions into the solution, but its ability to enhance Raman scattering is retained. However, it was noted that the enhanced spectra of *D*-alanine (Ala) dissolved in various buffers differed from each other and from the spectrum of amino acid crystallites [11].

The present work investigates surface enhanced Raman spectra of amino acids *D*-alanine and *DL*-serine (Ser) and their mixture on SNF, immersed in standard PBS solutions at 1 mM amino acid concentrations.

2. Materials and Methods

SNF which are ensembles of silver nanoparticles randomly distributed over glass surface were prepared by doping a soda-lime glass slide (Agar Scientific Ltd., Essex, UK) with silver ions via silver-to-sodium ion-exchange and annealing the silver-containing glass in a hydrogen atmosphere [10]. For the ion-exchange we immersed the slide for 20 min in $\text{AgNO}_3\text{-NaNO}_3$ melt containing 5 wt.% of AgNO_3 (LenReactiv, St. Petersburg, Russia) heated to 325 °C. The annealing in hydrogen was performed for 15 min at 250 °C.

Ala and Ser (pure grade, Reakhim, Moscow, Russia) in the form of both powders (crystallites) and 1 mM solutions in PBS, pH 7.4 (Biolot, St. Petersburg, Russia), were studied using confocal Raman microscope (Alpha 300R, Witec, Germany) equipped with 532 nm excitation laser (output power of ~30 mW) and 10×/0.25 objective (excitation spot diameter ~3 μm). The spectra were collected from the crystallites placed on the surface of SNF and glass and from the SNF/glass surface during their immersion in the solutions. In the last case, the glass slides with/without SNF were placed face up in a cuvette filled up with ~5 ml of the solution at ambient temperature (~20 °C), and the spectra were collected in the close vicinity of SNF/glass surface in different positions on the samples surface (~300 spectra). Each measured spectrum corresponded to an accumulation time of 1 s.

For peak detection, each spectrum of the data matrix, obtained by scanning the surface of the sample, was subjected to Savitzky-Golay smoothing and the baseline was removed using the rolling ball algorithm. Peak positions were calculated using the local maximum method, as implemented in OriginLab®. Peaks whose positions differed by less than $\pm 5\text{ cm}^{-1}$ were considered as one peak with the position of the most pronounced peak. For peak intensity analysis, cosmic spikes and baseline were removed from each spectrum using PALS algorithm with smoothness parameter 10^5 [12] and then subjected to standard principal component

analysis (PCA). Outlier spectra (1-3 spectra per dataset, presumably corresponding to SNF defects) were assessed manually and omitted from further analysis.

3. Results and discussion

The Raman spectra of Ala and Ser crystallites placed on SNF coincided with the spectra on glass without SNF, the spectra also completely matched the respective Ala and Ser reference spectra presented in literature [13]. At the same time, SNF immersed in PBS solutions showed spectra that were different from ones obtained for crystallites, and no measurable signal was obtained when a glass without silver nanoislands was immersed in PBS solutions of amino acids. This firmly indicated that, for the case of data collection from a PBS solution, the observed Raman signal is produced by amino acid molecules, adsorbed on SNFs.

The similarity of the spectra of crystallites placed on glass and SNF is because the size of crystallites is $\sim 100\ \mu\text{m}$, and the contribution to Raman scattering from molecules in the bulk of amino acids crystallites, which are not bound to SNF dominates over the Raman signal from several layers of molecules bound to SNF. When glass with/without SNF is immersed in PBS solutions, only a small fraction of molecules are adsorbed on the SNF/glass surface, and due to the extremely low Raman scattering cross-section of amino acid molecules in an aqueous environment [14], whose spectrum can only be detected in the case of enhanced Raman scattering provided by SNF. Thus, for the spectra obtained from PBS solutions, the Raman signal is generated by amino acids molecules bound to SNF.

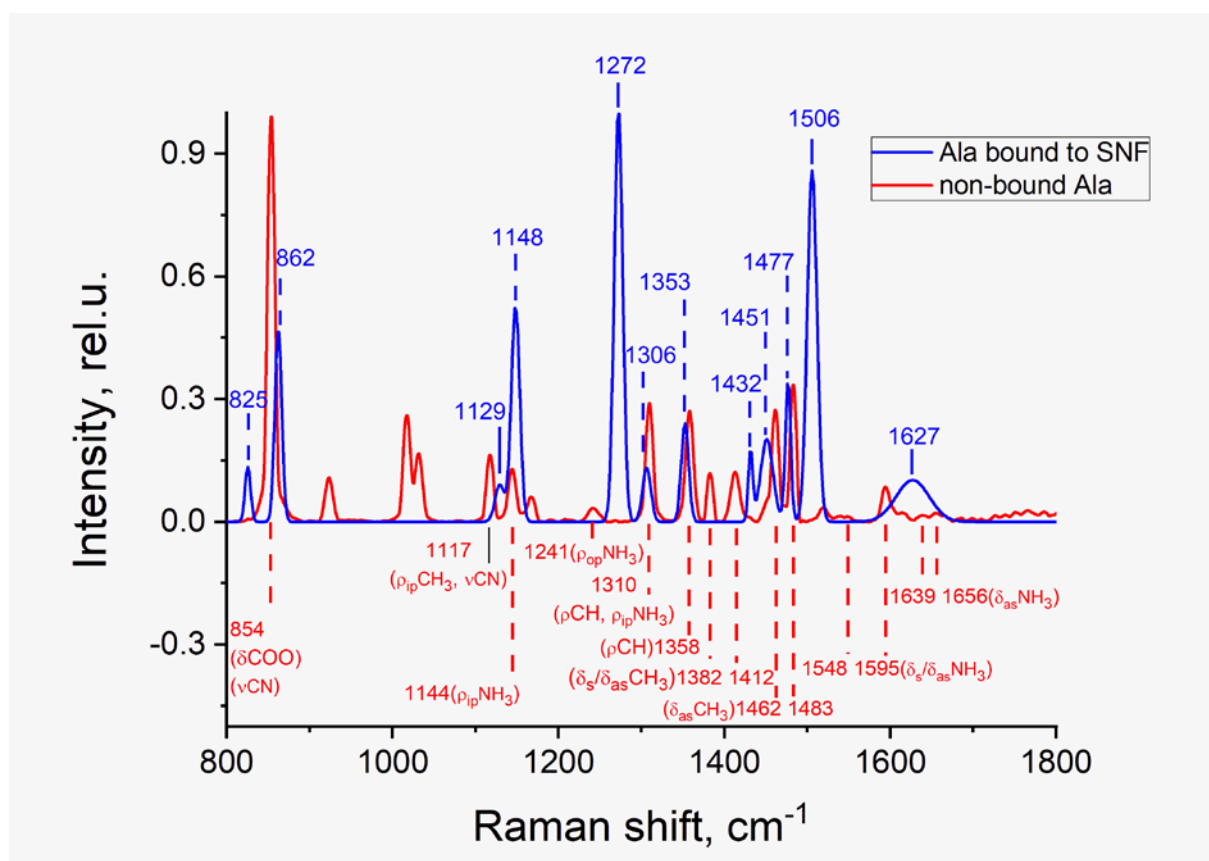


Figure 1. Comparison of Raman spectra of Ala bound to SNF (blue) and non-bound (crystallite) Ala (red). The peaks of crystallite spectrum are assigned to vibration

modes of C-N, NH₃ and CH₃ units: ν -stretching, δ -scissoring, ρ -rocking (ip – in plane, op – out of plane) [15]. The presented refined spectra were obtained by fitting the Gaussian peaks to the respective averaged spectra.

The comparison of averaged Raman scattering spectra of non-bound Ala and Ala bound to SNF is presented in Figure 1. The peaks in the spectrum of non-bound Ala are assigned to vibration modes of Ala crystallites in accordance with reference [15]. One can see in Figure 1 that the spectrum of Ala bound to SNF differs from the reference spectra of Ala crystallites. This difference is much more profound than the difference between the spectra of crystallites and published spectra of concentrated aqueous solutions (these spectra are relatively similar for alanine) [13]. Most peaks assigned to vibration modes of C-N, NH₃ and CH₃ are shifted, while peaks at 923 and 1017 cm⁻¹ assigned to vibration modes of COO [16] and C-C are missing. Due of strong shifts, the assignment is not unambiguous, but it clearly indicates that the binding mostly leads to a shift and enhancements of the peaks corresponding to NH₃. On the contrary, in the SERS spectra there are no peaks corresponding to COO.

To evaluate the stability and uniformity of the signal of Ala molecules adsorbed on SNF we performed a scanning of SNF surface with a time step of 1 s. The spectrum appeared immediately after the SNF was immersed in Ala solution and did not change with time. This suggests that not only the signal to noise ratio of a single run was low, but also the individual peaks of bound Ala were firmly detected (Figure 2a). The first principal component (PC1) of the data matrix corresponded to ~25% of the total variance, its loading matched the average spectrum, while the loadings of higher order PCs had no spectral features. Thus, there was only one significant spectrum, which was observed from all points of the sample, no dependence on time or position were detected. So, we can conclude that *D*-alanine binds to SNF rather rapidly, no slow change takes place, and only one mode of binding could be observed (the latter, however, may be an average of fast processes).

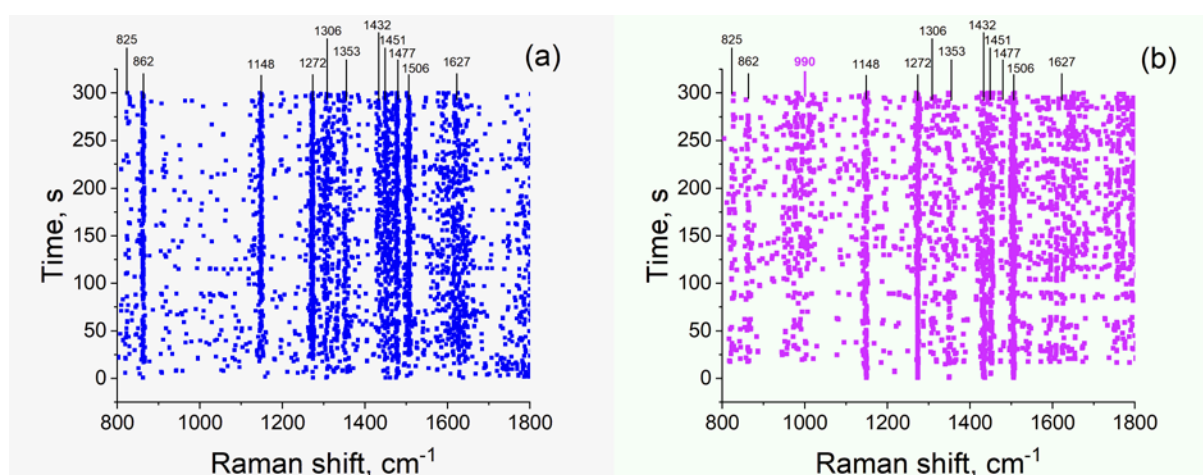


Figure 2. Raman peaks positions maps for (a) Ala and (b) Ser bound to SNF in PBS. Each point on the map corresponds to a feasible peak in the respective spectrum, as detected by the local maximum method.

Evaluation of Ser, bound to SNF in PBS, produces similar results (Figure 2b). Except for 800-1000 cm^{-1} region, the spectra of bound Ala and Ser are quite similar. In fact, they are more similar to each other in terms of peak positions and relative intensities than to the spectra of the respective crystalline states (see Figure 3a). The Ser spectrum has only one additional weak peak at 990 cm^{-1} , which can be attributed to C-N stretching [17]. The first principal component corresponds to ~60% of total variance of the data matrix, and other components are effectively noise. The principal spectrum of Ser bound to SNF is apparently simpler than the spectrum of bound Ala, despite the fact that Ala is chemically simpler. This may be a result of peak splitting and their disappearance in noise, alternatively it may be a result of some kind of additional ordering by intermolecular interaction (see below). The overall Raman signal for bound Ser was stronger than for bound Ala but it displayed large irregular point-to-point variations (up to 10-fold changes in PC1 scores were observed).

These observations indicate that the binding of Ala and Ser molecules to silver surface is structurally similar and highly polarized. Due to the presence of 0.13 M of chloride in PBS, which strips part of silver as Ag(I) into chlorocomplexes in the solution, silver nanoislands in PBS contain excess electrons and gain an effective negative charge. At pH 7.4, which can be assumed constant because of large buffer capacity of PBS, Ala or Ser molecules exist predominantly in neutral zwitterionic state, similar to crystal state or concentrated solutions. So, it is highly feasible that amino acid zwitterions orient themselves with positively charged NH_3 group towards the surface and negative COO group away from it. Because of this, the peaks associated with NH_3 group vibrations are most strongly affected by the local plasmons of metal surface, while the other vibrations have an unfavorable orientation and/or are not insufficiently enhanced. Potential protonation of carboxylate group on binding (which is highly improbable at pH 7.4 but cannot be ruled out) does not interfere with the assumed orientation. As Ala and Ser are simple and differ only by a single group, the similarity of binding and enhancements is very tenable. Analogous effects were observed for other amino acids, which hint for strong electrostatic orientation of α -aminocarboxylic group by silver surface [18]. It should be noted that the presence of chloride, which decreases the electrochemical potential of the silver nanoparticles (standard redox potential for silver $E^\circ \sim 0.25$ V in PBS), is important for tight binding. When SNF was immersed in distilled water ($E^\circ \sim 0.8$ V) no Raman peaks were observed even with 0.1 M solutions of Ala and Ser (data not shown).

To test the ability to detect both amino acids in the mixture we examined Raman spectra collected in the vicinity of SNF immersed in the solution, containing 1 mM Ala and 1 mM Ser in PBS. The relative intensities of Raman signals can be seen from principal spectra in Figure 3a. The peaks positions map is shown in Figure 3b. Although the spectrum of the mixture on SNF and the spectra of the individual amino acids (bound and non-bound) has some common peaks and features, the response is far from additive and significant redistribution of intensities and appearance of new peaks can be seen (Figure 3a). The spectrum of the mixture is also time- and position-independent, see Figure 3b (PC1 corresponded to 45% of total variance; PC2 comprised less than 2%, PC2 “spectrum” did not contain any characteristic Raman peaks). Total signal to noise ratio and point to point variations in the spectrum of the mixture are smaller than in bound Ser spectra and similar to that of bound Ala.

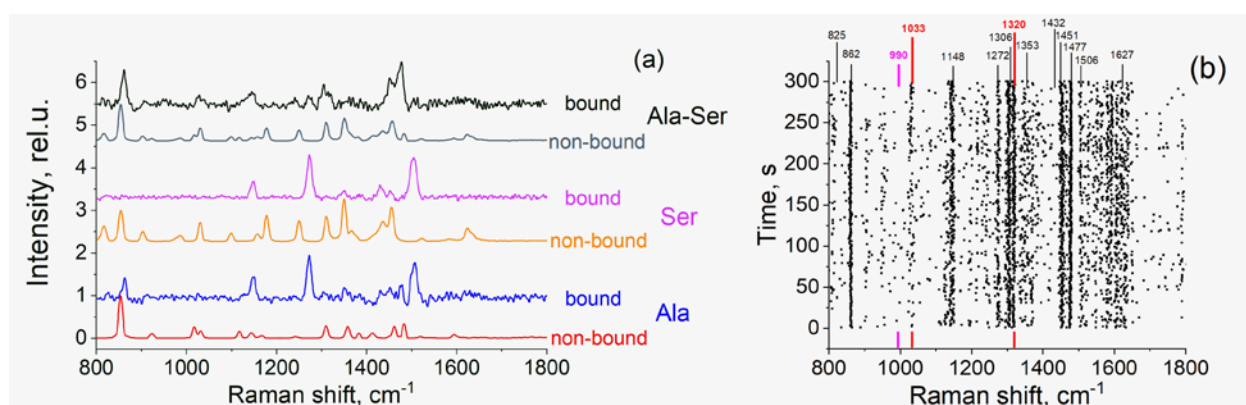


Figure 3. (a) Most significant spectral contributions (PC1 loadings) in the data matrices of Raman spectra of bound to SNF in PBS and the spectra of non-bound (crystallite) Ala, Ser and 1:1 Ala-Ser mixture (theoretical sum). (b) Raman peaks positions map for Ala-Ser mixture: black labels– Ala and Ser common peaks, magenta labels – Ser only peak, red labels– Ala-Ser only peaks.

Summarizing these data, we can conclude that serine and alanine molecules adsorb on silver nanoislands simultaneously with comparable affinity, forming a hybrid molecular layer. This layer is different from layers formed by pure amino acids and has a significant contribution from Ala-Ser complexes resulting in specific pattern of peak intensities. The latter indicates significant interactions between adsorbed amino acids, which means that the layer of amino acid molecules on silver particles in the studied conditions is dense. Thus, non-covalent intermolecular interactions can make structural changes to the layers of oriented amino acids molecules on silver surface, and these changes are strong enough to manifest in the positions and intensities of enhanced Raman peaks. This is quite dissimilar to solution studies, as specific non-covalent interaction of amino acids in the bulk aqueous media at the studied concentrations is negligible, and the spectral responses are generally additive [19]. While this finding is not beneficial to quantitative analytical applications, as it makes the calibration and rational spectral analysis more complicated, it is highly interesting for the studies of non-covalent intermolecular interactions of organic molecules in thin layers in aqueous environment.

4. Conclusion

We have shown that enhanced Raman spectra of *D*-alanine and *DL*-serine can be reliably observed using Raman microscopy from silver nanoisland films immersed in standard PBS solutions with millimolar concentrations of the amino acids. The obtained spectra significantly differ in peak intensities and positions from Raman spectra of bulk solutions and crystallites of the corresponding amino acids on SNFs and on glass. The effect is tentatively attributed to electrostatic orientation of amino acid zwitterions by silver nanoparticles, which acquire a negative charge because of Ag(I) stripping by chloride in the solution, as the enhancement vanished if distilled H₂O was used instead of PBS. The spectrum from SNF in amino acids mixture is not additive which indicates a strong interaction of alanine and serine molecules at SNF surface. While the spectra can be used to roughly discriminate pure amino

acids and mixture, multivariate calibration would not be easy, because the generalized Beer's law is not satisfied for the mixture.

On the other hand, the observed effects may be used to study molecular properties and intermolecular interactions at a silver nanoparticle surface, which are negligible or too transient in the bulk solution. It is also important that the effective charge of SNF can be adjusted by changing the concentration of Ag(I)-stabilizing ligands (e.g. chloride) in the solution, providing an additional controlled parameter.

Acknowledgements

AS and VZh thank the support by Ministry of Education and Science of the Russian Federation as a part of the State program for the fundamental research (theme code FSEG-2020-0024). GY thanks the support by the National Natural Science Foundation of China (No. 52072231) and the Presidential Foundation of the China Academy of Engineering Physics (YZJLX2019011).

Author Contributions

Conceptualization, A.L.; Methodology, A.S.; Investigation, E.B., A.R., and G.Y.; Resources, V.Zh.

Conflicts of Interest

The authors declare no conflict of interest.

References

1. Kneipp, K.; Kneipp, H.; Itzkan, I.; Dasari, R.R.; Feld, M.S. Surface-enhanced Raman scattering and biophysics. *J. Phys. Condens. Matter* **2002**, *14*, 202, doi:10.1088/0953-8984/14/18/202.
2. Kuttner, C. Plasmonics in Sensing: From Colorimetry to SERS Analytics. In *Plasmonics*; IntechOpen, **2018**; p. 252.
3. Raschke, G.; Kowarik, S.; Franzl, T.; Sönnichsen, C.; Klar, T.A.; Feldmann, J.; Nichtl, A.; Kürzinger, K. Biomolecular recognition based on single gold nanoparticle light scattering. *Nano Lett.* **2003**, *3*, 935–938, doi:10.1021/nl034223+.
4. Choe, A.; Yeom, J.; Shanker, R.; Kim, M.P.; Kang, S.; Ko, H. Stretchable and wearable colorimetric patches based on thermoresponsive plasmonic microgels embedded in a hydrogel film. *NPG Asia Mater.* **2018**, *10*, 912–922, doi:10.1038/s41427-018-0086-6.
5. Zopf, D.; Jatschka, J.; Dathe, A.; Jahr, N.; Fritzsche, W.; Stranik, O. Hyperspectral imaging of plasmon resonances in metallic nanoparticles. *Biosens. Bioelectron.* **2016**, *81*, 287–293, doi:10.1016/j.bios.2016.03.001.
6. Graff, M.; Bukowska, J. Surface-enhanced Raman scattering (SERS) spectroscopy of enantiomeric and racemic methionine on a silver electrode-evidence for chiral discrimination in interactions between adsorbed molecules. *Chem. Phys. Lett.* **2011**, *509*, 58–61, doi:10.1016/j.cplett.2011.04.089.
7. Zhurikhina, V. V.; Brunkov, P.N.; Melehin, V.G.; Kaplas, T.; Svirko, Y.; Rutckaia, V.

- V.; Lipovskii, A.A. Self-assembled silver nanoislands formed on glass surface via out-diffusion for multiple usages in SERS applications. *Nanoscale Res. Lett.* **2012**, *7*, 1–5, doi:10.1186/1556-276X-7-676.
8. Babich, E.; Scherbak, S.; Asonkeng, F.; Maurer, T.; Lipovskii, A. Hot spot statistics and SERS performance of self-assembled silver nanoisland films. *Opt. Mater. Express* **2019**, *9*, 4090, doi:10.1364/OME.9.004090.
 9. Babich, E.; Redkov, A.; Reduto, I.; Lipovskii, A. Self-Assembled Silver-Gold Nanoisland Films on Glass for SERS Applications. *Phys. status solidi - Rapid Res. Lett.* **2018**, *12*, 1700226, doi:10.1002/pssr.201700226.
 10. Skvortsov, A.; Babich, E.; Redkov, A.; Lipovskii, A.; Zhurikhina, V. Stable in Biocompatible Buffers Silver Nanoisland Films for SERS. *Biosensors* **2021**, *11*, 448, doi:10.3390/bios11110448.
 11. Zhurikhina, V.; Skvortsov, A.; Babich, E.; Redkov, A. Raman Spectroscopy of Amino Acids Using Metal Nanoisland Films on Glass. In Proceedings of the 2021 International Conference on Electrical Engineering and Photonics (EExPolytech); IEEE, 2021; pp. 168–170.
 12. Baek, S.-J.; Park, A.; Ahn, Y.-J.; Choo, J. Baseline correction using asymmetrically reweighted penalized least squares smoothing. *Analyst* **2015**, *140*, 250–257, doi:10.1039/C4AN01061B.
 13. Zhu, G.; Zhu, X.; Fan, Q.; Wan, X. Raman spectra of amino acids and their aqueous solutions. *Spectrochim. Acta Part A Mol. Biomol. Spectrosc.* **2011**, *78*, 1187–1195, doi:10.1016/j.saa.2010.12.079.
 14. Gaff, J.F.; Franzen, S. Excited-State Geometry Method for Calculation of the Absolute Resonance Raman Cross Sections of the Aromatic Amino Acids. *J. Phys. Chem. A* **2009**, *113*, 5414–5422, doi:10.1021/jp809431k.
 15. Chowdhry, B.Z.; Dines, T.J.; Jabeen, S.; Withnall, R. Vibrational Spectra of α -Amino Acids in the Zwitterionic State in Aqueous Solution and the Solid State: DFT Calculations and the Influence of Hydrogen Bonding. *J. Phys. Chem. A* **2008**, *112*, 10333–10347, doi:10.1021/jp8037945.
 16. Hernández, B.; Pflüger, F.; Nsangou, M.; Ghomi, M. Vibrational Analysis of Amino Acids and Short Peptides in Hydrated Media. IV. Amino Acids with Hydrophobic Side Chains: L-Alanine, L -Valine, and L -Isoleucine. *J. Phys. Chem. B* **2009**, *113*, 3169–3178, doi:10.1021/jp809204d.
 17. Jarmelo, S.; Carey, P.R.; Fausto, R. The Raman spectra of serine and 3,3-dideutero-serine in aqueous solution. *Vib. Spectrosc.* **2007**, *43*, 104–110, doi:10.1016/j.vibspec.2006.06.021.
 18. Graff, M.; Bukowska, J. Enantiomeric recognition of phenylalanine by self-assembled monolayers of cysteine: Surface enhanced Raman scattering evidence. *Vib. Spectrosc.* **2010**, *52*, 103–107, doi:10.1016/j.vibspec.2009.11.003.
 19. Candeloro, P.; Grande, E.; Raimondo, R.; Di Mascolo, D.; Gentile, F.; Coluccio, M.L.; Perozziello, G.; Malara, N.; Francardi, M.; Di Fabrizio, E. Raman database of amino acids solutions: a critical study of Extended Multiplicative Signal Correction. *Analyst* **2013**, *138*, 7331, doi:10.1039/c3an01665j.